A Modular Approach for Three-Dimensional Shape Optimization of Structures

R. J. Yang* and M. E. Botkin†
General Motors Research Laboratories, Warren, Michigan

An approach for shape optimization of three-dimensional solid structures is described. A major consideration in the development of this capability was the desire to use a commercially available finite-element program, such as NASTRAN, for analysis. Since NASTRAN cannot be called a subroutine, a system architecture of independently executable modules was developed, in which sequential execution is controlled by job control language. Also, sensitivities are not commonly available in commercial programs. A material derivative approach was developed to obtain shape sensitivities by postprocessing finite-element boundary stresses stored on files. A parameterized surface description and mesh generation are provided using isoparametric mapping patches. The feasible directions algorithm CONMIN is used for optimization. Several automotive-related examples are used to evaluate the program's effectiveness.

Introduction

ONLY a limited amount of work has been accomplished in three-dimensional shape optimization using solid finite-element analysis.[1,2] A new modular approach to the development of such a capability is described in this paper. It was desired to have a system that uses a commercial finite-element code as the analysis capability because of its widespread acceptance by the structural analysis community. There were two drawbacks to achieving this goal. Most commercial finite-element codes cannot be used as a subroutine and do not have the capability to provide design sensitivities for shape variables. The first problem was addressed by building a system of independently executable program modules in which the overall execution was controlled by a higher-level system language. The second problem was handled through the use of a recently developed technique for obtaining shape design sensitivities,[3-6] which does not require the finite-element source program to be modified. These two capabilities are the basis for allowing the use of a variety of structural analysis programs (NASTRAN, ANSYS, SAPIV, etc.) to be used with a relatively small amount of additional program development.

In this study, NASTRAN was used for analysis. The shape design element concept[7] and a generic modeling technique[1,2] were used to associate design variables with surface movement and the finite-element mesh. The initial generic model can be conveniently created using a technique[8] that allows solid models to be created by specifying the boundary surfaces.

Three design examples were used to demonstrate the use of the program. A three-dimensional beam that has an exact solution based on classical simple beam theory was used to validate the system. An engine bearing cap problem was chosen as the second example. The third problem was an idealized engine connecting rod.

Presented as Paper 86-1009 at the AIAA/ASME/ASCE/AHS 27th Structures, Structural Dynamics and Materials Conference, San Antonio, TX, May 19–21, 1986; received June 5, 1986; revision received Aug. 25, 1986.

*Senior Research Engineer, Engineering Mechanics Department.
†Senior Staff Research Engineer, Engineering Mechanics Department.

Design Sensitivity Analysis

The variational design sensitivity theory uses the material derivative concept of continuum mechanics and an adjoint variable method to obtain computable expressions for the effect of shape variation on the functionals arising in the shape design problem. The design sensitivities of performance functionals are essential in structural optimization. Once those derivatives are calculated, one can use any optimization technique to obtain a better design.

The variation of displacement functional ψ with respect to shape change is derived by differentiating the variational equilibrium equation and employing the adjoint variable method, to obtain[3-5]

$$\delta\psi = \int_\Gamma \sigma^{ij}(z)\,\epsilon^{ij}(\lambda)\,V^T n\,d\Gamma \tag{1}$$

where ψ is defined by

$$\psi = \int_\Omega z\delta(x-\bar{x})\,d\Omega \tag{2}$$

in which $\bar{x}$ is the point of interest, δ the Dirac measure at zero, Ω the physical domain; σ^{ij} and ϵ^{ij} are the stress and strain tensors, respectively; V is the design perturbation, which can be thought of as velocity, and n is the unit normal vector of moving boundary Γ. The vectors of z and λ are the displacement vectors for state and adjoint equations, respectively, which can be expressed as follows:

$$\int_\Omega \sigma^{ij}(z)\,\epsilon^{ij}(\bar{z})\,d\Omega = \int_{\Gamma^2} T_i \bar{z}_i\,d\Gamma \tag{3}$$

$$\int_\Omega \sigma^{ij}(\lambda)\,\epsilon^{ij}(\bar{\lambda})\,d\Omega = \int_\Omega \delta(x-\bar{x})\bar{\lambda}\,d\Omega \tag{4}$$

where T_i is a traction vector, Γ^2 is a loaded boundary, and (-) indicates the virtual displacements that satisfy the kinematically admissible displacement field. One should notice that in Eq. (1) the kinematically constrained boundary and loaded boundary are assumed to be fixed and that the variation of the displacement functional is affected only by the normal movement of the boundary of the physical domain. Physically, the adjoint equation of Eq. (4) is interpreted as applying a unit load at the point $\bar{x}$, where the displacement is of interest.

The stress variation also can be derived in the same ways, except that the Dirac measure cannot be used because of the discontinuity of the stresses along the interelemental boundaries. A characteristic function, which averages stress over a small region, is introduced to treat stress constraints in Refs. 5 and 9. The variation of stress functional over a small region Ω_p then is derived as

$$\delta\psi = \int_\Gamma \sigma^{ij}(z)\,\epsilon^{ij}(\lambda)\,V^T n\,d\Gamma + m_p \int_{\Gamma_p} (\phi - \psi)\,V^T n\,d\Gamma \quad (5)$$

where ϕ is a function of stresses, Γ_p is the boundary of Ω_p, and the characteristic function m_p, the constraint functional ψ, and the adjoint load equation are defined as follows:

$$m_p = \frac{1}{\int_{\Omega_p} d\Omega}, \qquad \text{in } \Omega_p$$

$$= 0, \qquad \text{in } \Omega - \Omega_p \quad (6)$$

$$\psi = \int_\Omega \phi[\sigma(z)]\,m_p\,d\Omega \quad (7)$$

$$\int_\Omega \sigma^{ij}(\lambda)\,\epsilon^{ij}(\bar{\lambda})\,d\Omega = \int_\Omega \frac{\partial\phi}{\partial\sigma^{ij}}(z)\,\sigma^{ij}(\bar{\lambda})\,m_p\,d\Omega \quad (8)$$

Parameterizing design change V of Eq. (5), one obtains

$$\frac{\partial\psi}{\partial b}\delta b = \int_\Gamma \sigma^{ij}(z)\,\epsilon^{ij}(\lambda)\,n^T\frac{\partial r}{\partial b}\delta b\,d\Gamma + m_p\int_{\Gamma_p}(\phi - \psi)\,n^T\frac{\partial r}{\partial b}\delta b\,d\Gamma \quad (9)$$

where r and b are position and shape design variable vectors, respectively. Since Eq. (9) is linear in δb, one can eliminate δb to obtain the sensitivity formula as

$$\frac{\partial\psi}{\partial b} = \int_\Gamma \sigma^{ij}(z)\,\epsilon^{ij}(\lambda)\,n^T\frac{\partial r}{\partial b}\,d\Gamma + m_p\int_{\Gamma_p}(\phi - \psi)\,n^T\frac{\partial r}{\partial b}\,d\Gamma \quad (10)$$

Since the averaged stress is applied over an element in finite-element analysis, this implies that small elements should be used in areas of high stress or stress concentration. It was shown in Ref. 9 that undesirable shapes may be obtained when elements are too big or distorted in a highly stressed area.

Alternately, one may use the definition of stress computation in finite-element analysis to obtain the stress gradient at a point. The elemental stresses are computed by using the following equation:

$$\sigma = DBz^e \quad (11)$$

where D is the elasticity matrix, B the strain recovery matrix that contains the derivatives of shape functions, and z^e an elemental displacement vector. Differentiating Eq. (11) with respect to the design variables, one obtains

$$\sigma_i' = D\left(Bz_i^{e\prime} + B_i' z^e\right) \quad (12)$$

where the subscript i with a prime superscript indicates the derivative with respect to the ith design variable. Notice that the first term on the right side of Eq. (12) is only a combination of displacement gradients and can be obtained by applying a combined adjoint load to the system and using the same formula of Eq. (1). In fact, one can show that Eq. (12) is equivalent to Eq. (9) when the domain Ω_p shrinks to a point.

First of all, assume the stress function ϕ as stress vector σ; then, the constraint functional ψ is equivalent to the average stress vector $\bar{\sigma}$ over Ω_p. Let Ω_p shrink to a point $\bar{x}$; the adjoint equation (8) then becomes

$$\int_\Omega \sigma^{ij}(\lambda)\,\epsilon^{ij}(\bar{\lambda})\,d\Omega = \int_\Omega \delta(x - \bar{x})\,DB\bar{\lambda}\,d\Omega \quad (13)$$

Comparing with Eq. (12), this equation verifies that the adjoint load for stress constraint functional is only a combined adjoint load for displacement constraint functional and that the first terms of Eqs. (9) and (12) are equivalent. The second term of Eq. (9) can be parameterized and simplified by using the divergence theorem as

$$m_p\int_{\Gamma_p}(\sigma - \bar{\sigma})\,n^T\frac{\partial r}{\partial b}\,d\Gamma = m_p\int_{\Omega_p}\nabla\cdot(\sigma - \bar{\sigma})\frac{\partial r}{\partial b}\,d\Omega$$

$$m_p\int_{\Gamma_p}(\sigma - \bar{\sigma})\,n^T\frac{\partial r}{\partial b}\,d\Gamma = m_p\int_{\Omega_p}(\sigma - \bar{\sigma})\nabla\cdot\left(\frac{\partial r}{\partial b}\right) + \nabla\sigma\cdot\left(\frac{\partial r}{\partial b}\right)d\Omega \quad (14)$$

Note that the first term of Eq. (14) is the effect of area change for the average stress constraint functional and that this term vanishes when the area of the element approaches zero. The second term of Eq. (14) can be further simplified as

$$m_p\int_{\Omega_p}\frac{\partial x_i}{\partial b}\frac{\partial\sigma}{\partial x_i}\,d\Omega = m_p\int_{\Omega_p}\frac{\partial\sigma}{\partial b}\,d\Omega = m_p\int_{\Omega_p} D\frac{\partial B}{\partial b}z^e\,d\Omega \quad (15)$$

since the partial derivative is applied for field variables only. If Ω_p shrinks to a point, Eq. (15) converges to the second term of Eq. (12). This completes the proof of equivalence of Eqs. (9) and (12).

Another way of looking at the material derivative formulation is to take the pointwise material derivative of stress (if it exists) at $x \in \Omega$ in the same way as of displacement as

$$\delta\sigma = \frac{\partial\sigma}{\partial\tau} + \nabla\sigma\cdot V$$

or

$$\frac{\partial\sigma}{\partial b}\delta b = \left(DB\frac{\partial z}{\partial b} + D\frac{\partial B}{\partial b}z\right)\delta b \quad (16)$$

The first term of Eq. (16) is the change due to time τ or design for a fixed isolated point x and corresponds to the first term of Eq. (12) while the second term is the stress change due to position change and is equivalent to the second term of Eq. (12). This confirms that theoretically, these two approaches are equivalent. One should note that although these two equations are equivalent, Eq. (9) is based on variational theory while Eq. (12) is not, but it is meaningful in a practical sense.

The primed matrix of the second term of Eq. (12) can be evaluated from the derivative of the nodal coordinates with respect to shape design parameters.[10] It can be computed analytically, or by using a finite-difference method. In this study, analytical derivatives are used for B'.

The characteristic function stress-averaging strategy for stress design sensitivity analysis[5,9] is similar to using the element center as the stress constraint point, while the approach described here makes it possible to have as many stress constraint points as desired in an element. It has an advantage especially when large stress variation over an element occurs, since the averaging stress strategy may lead to a misleading

constraint value and result in an undesirable shape.[9] In this paper, the eight corner points of the solid element are chosen as the stress constraint points.

Modularized System

The modularized system comprises a mesh generator; the finite-element code, NASTRAN; the adjoint load and constraints definition program; a design sensitivity analysis module; and an optimization module, CONMIN. Each of these is an independent program and is treated as a module. The flowchart of the system is shown in Fig. 1. Initially, one has to generate a generic model for the structural component and create a NASTRAN data deck for the NASTRAN run. The whole cycle of the system proceeds as follows: run the NASTRAN code for the actual load; calculate the cost function, constraints, and adjoint loads using the NASTRAN output; rerun the NASTRAN code for the adjoint loads; and perform the design sensitivity analysis and optimization to obtain a new design. Finally, a new finite-element mesh and NASTRAN data deck for the new design are generated.

The generic model for a structural component is generated by using the MAGIC three-dimensional mesh generator,[8] since the surface definition is very convenient in this program. An isoparametric mapping mesh generator[1,2] is then used to generate the necessary finite elements for the NASTRAN code. It is clear that these two steps can eventually be combined, once a more sophisticated mesh generator is available.[11]

The MSC/NASTRAN version 63 finite-element code is employed for analysis. The new feature of the NASTRAN data base is used to save computing time for reanalysis of the adjoint loads. This data base, created by the first NASTRAN run, preserves the stiffness and boundary-condition information and results in easier input data preparation and less computing time for the reanalysis.The reanalysis, using the data base, is much cheaper than the first analysis. For the engine connecting rod (example) that has 2126 degrees of freedom, the reanalysis costs only about 5% of the first analysis.

The displacements, stresses, and geometric information needed for design sensitivity calculation are obtained by using an ALTER feature in NASTRAN to write that information on a file for postprocessing.

The ADJLOD module is used to define the cost function and constraints for the design problem and to calculate the adjoint loads for the constraints that are active or violated. The displacements, stresses, and geometric information from the NASTRAN output are first read to define the constraints for the structural component. A NASTRAN deck containing the adjoint loads is then created for reanalysis.

The SENSTY module performs the design sensitivity analysis for the cost and the active constraints, and then performs the optimization process by calling the optimizer CONMIN as a subroutine. CONMIN is based on Zoutendijk's feasible direction method and was developed by Vanderplaats.[12] Before executing the module, the NASTRAN output files for the actual load and the adjoint loads should be available. The module then changes the design and creates new input data for the MESHGN module, which will generate a new mesh and a new NASTRAN data file for the next design iteration, if necessary.

The termination condition for the optimization process is set up in module SENSTY by using a return code. The code is interpreted by IBM job control language (JCL) in which the COND function is used to decide if the process is to be continued or stopped. If another iteration is required, the JCL will resubmit itself.

Table 1 Design variables for simple beam

No.	Initial, mm	Final, mm	Lower bound, mm	Upper bound, mm
1	8.0	5.0061	0.1	10.0
2	8.0	3.6186	0.1	10.0
3	8.0	1.4403	0.1	10.0

Numerical Examples

Three-Dimensional Beam

Figure 2 represents a three-dimensional beam design example for which the dimensions, loading, and constraint conditions are shown. An exact solution for the optimum shape, assuming beam theory, exists. The left end of the beam is clamped, and a concentrated load of 10,000 MPa is applied at the right end. The upper and lower surfaces of the beam, parallel to the x-z plane, are to be varied. Considering symmetry and constant width (z dimension) conditions, the shape of curve ABC determines the shape of the whole beam. Thus, the optimal design problem is to find the shape of the beam that will minimize the total volume, such that the bending stresses are less than the maximum allowable value.

The generic model for the beam with only one element is shown in Fig. 2. The key dimensions considered as design variables are the heights of A, B, and C, calculated from the central plane. A 20-node isoparametric element is employed for analysis. The isoparametric model, shown in Fig. 3, contains 68 nodal points, 5 finite elements, and 180 degrees of freedom. Young's modulus, Poisson's ratio, and allowable bending stress are 10.0×10^6, 0.3, and 3000 Mpa, respectively.

The initial design is chosen as a flat surface and is shown in Table 1. Initially, the volume is 8000 mm^3 with no stress violation. After 10 design iterations, it is reduced to 3487.0 mm^3 with 3.7% stress violation, which could be reduced further by continuing the optimization process; however, it is tolerable in an engineering sense. The final design variables are also shown in Table 1. The final shape, shown in Fig. 3, is very close to the analytical solution and the result obtained by Imam.[1] Figure 4a shows the design history for this simple beam example. One observes that the convergence rate is quite good. At step 4, the cost is very close to the final value; however, it has 18% stress violation. Thus, the optimizer is

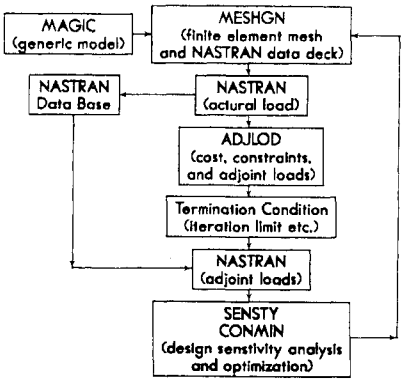

Fig. 1 Flowchart of modularized system.

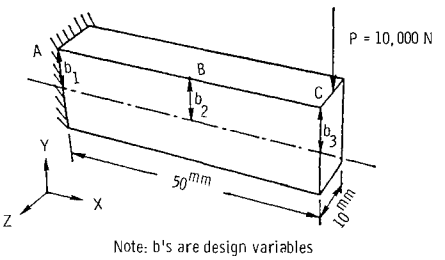

Fig. 2 Generic model of simple beam.

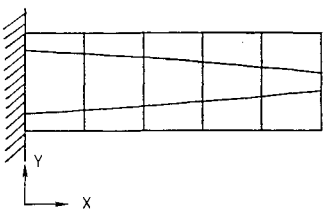

Fig. 3 Initial and final designs of simple beam.

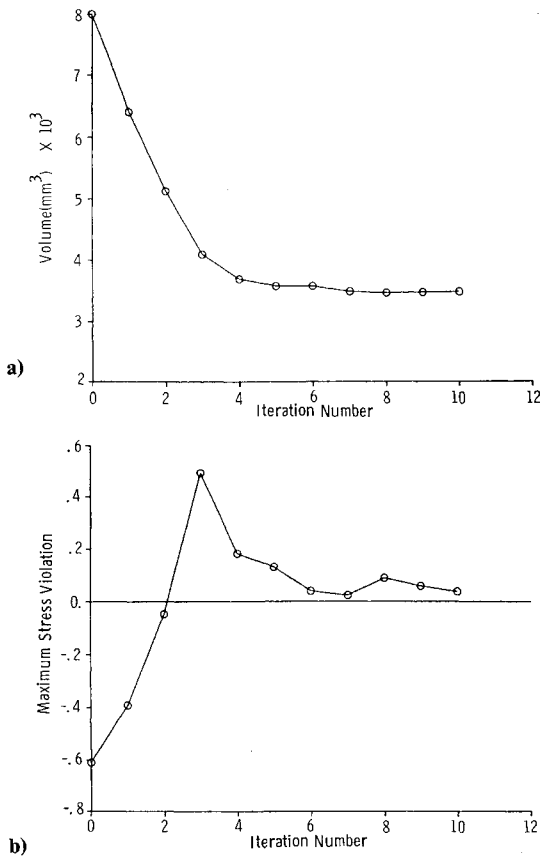

Fig. 4 Design histories of three-dimensional beam.

trying to force the design into the feasible region in the subsequent steps. The oscillating maximum stress violation history shown in Fig. 4b is due to function approximation by the use of Taylor's series expansion.

Engine Main Bearing Cap

An engine main bearing cap, subjected to a bolt load and oil film pressure and analyzed by Imam,[2] is used as the second example. The design problem is to find the minimum volume of the bearing cap that satisfies the distortion and stress constraints.

The bolt load, caused by the torque on the bolts, is a compressive load on the cap that is assumed to remain constant during the operation of the engine. The axial load of 53,400 N is estimated by an empirical equation[2] and is distributed equally to all the nodes on the circumference of each bolt hole whose radius is assumed as 6.35 mm.

The oil film pressure is a radial pressure load on the bearing surface. For a given crank angle, the film pressure varies over the circumference of the bearing. Since the problem of determining accurate pressure profiles is not the main subject of this paper, a pressure profile used in Ref. 2, as shown in Fig. 5, is employed. The pressure load is modeled simply by

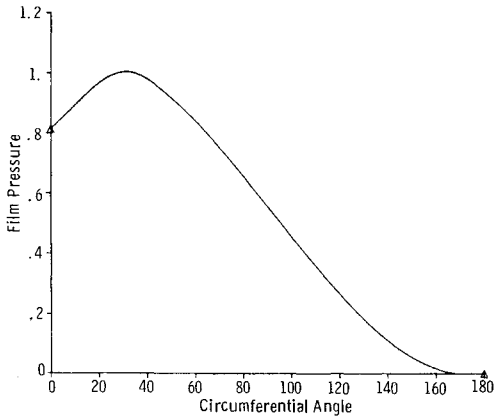

Fig. 5 Oil film pressure profile.

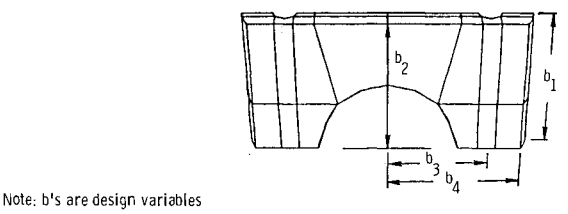

Fig. 6 Generic model of engine bearing cap.

distributing the total load of 24840 N in the y direction over the bearing surface in the ratio of the pressure at each point.

Since the bearing is often a cast-iron part, the failure occurs in the form of brittle fracture at the point of critical stress. A failure criterion for brittle fracture used in Ref. 2 is employed here, and it is expressed as

$$\tfrac{1}{2}\left[(\sigma_1-\sigma_2)^2+(\sigma_2-\sigma_3)^2+(\sigma_3-\sigma_1)^2\right] \le X_T X_C/S \quad (17)$$

where S is the factor of safety that may take into account the effect of fatigue and prestressing of the part, X_T the ultimate tensile strength, and X_C the ultimate compressive strength. One may notice that the criterion is similar to the von Mises yield criterion that is used for ductile material. This constraint will be applied to stresses calculated at each node on the finite-element model of the bearing cap except those points where the bolt loads are applied, since the stresses are not accurate because of the approximation of the bolt load as a concentrated load. The values of X_T, X_C and S used in this paper are 206.7 MPa, 751 MPa, and 2, respectively. Young's modulus and Poisson's ratio are 1.1×10^5 MPa and 0.3, respectively. The thickness of the bearing cap is assumed as a constant of 23.825 mm during the design process.

The displacement constraint for the bearing cap is imposed on any point of the bearing surface in the radial direction as

$$|u_r| \le 1/1000 \quad (18)$$

The purpose of imposing this constraint is to keep the distortion of the bearing surface to a minimum, so that good lubrication properties of the bearing result.

Using the symmetrical conditions, half the bearing cap is analyzed. The generic model and design parameters are shown in Fig. 6. In this model, four design variables are chosen to define the geometry of the bearing cap. The finite-element model, as shown in Fig. 7a, contains 136 solid elements, 1005 nodal points, and 2502 degrees of freedom.

The initial values of the design variables are listed in Table 2. Initially, the volume is 95,045 mm^3 with no constraint

Table 2 Design variables for engine bearing cap

No.	Initial, mm	Final, mm	Lower bound, mm	Upper bound, mm
1	73	62.9	25.4	76.2
2	73	62.588	40.64	76.2
3	53.975	55.367	47	57.15
4	73.025	68.844	65.405	78.105

Table 3 Design variables for engine connecting rod

No.	Initial, mm	Final, mm	Lower bound, mm	Upper bound, mm
1	10.956	12.512	0.1	100.0
2	6.37	2.8478	0.1	100.0
3	3.9667	1.4220	0.1	100.0
4	3.0024	1.0964	0.1	100.0
5	3.2711	1.2733	0.1	100.0
6	6.8156	7.2219	0.1	100.0
7	31.271	26.461	24.0	100.0
8	17.553	13.300	13.3	100.0

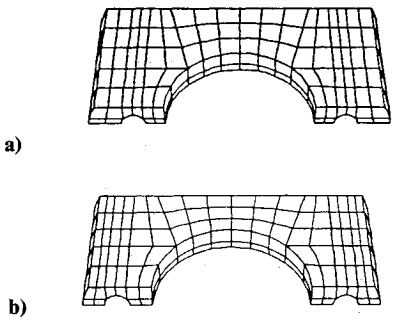

Fig. 7 Designs of engine bearing cap: a) initial, b) final.

violation. After four design iterations, it is reduced to 71,775 mm^3 with no constraint violation. This design has 18 constraints active, 12 for stress and 6 for displacement, if the constraint thickness parameter is chosen as 0.1. The design process is stopped because the cost function is unchanged after three iterations.

The final design variables and final shape are shown in Table 2 and Fig. 7b, respectively. Comparing to the initial design, one sees that the final design tends to reduce the heights and width of the bearing cap, while moving the bolt hole outward. Figure 8a shows the design history for the bearing cap, while Fig. 8b shows the maximum displacement and stress constraint histories.

Since Ref. 2 does not provide sufficient detailed information for the design and constraints, a precise comparison cannot be made.

Engine Connecting Rod

An idealized engine connecting rod, which connects the crank shaft and piston pin of an engine and transmits an axial compressive load during firing and a tensile load during the intake cycle of the exhaust stroke, is employed as the third example. Shape optimization of similar components have been studied by Yoo et al.[13] and Yang et al.,[14] assuming a plane stress state. However, a fully three-dimensional shape optimization for the connecting rod is still not available in the literature.

For simplicity, the right hole of the connecting rod that connects the piston pin is fixed to eliminate rigid body motion; and the arbitrarily selected pressure of 3000 MPa is applied to the left hole, from 0 to 90 deg, to simulate the firing forces. The von Mises stress constraint is imposed at each node in the finite-element model of the connecting rod. The

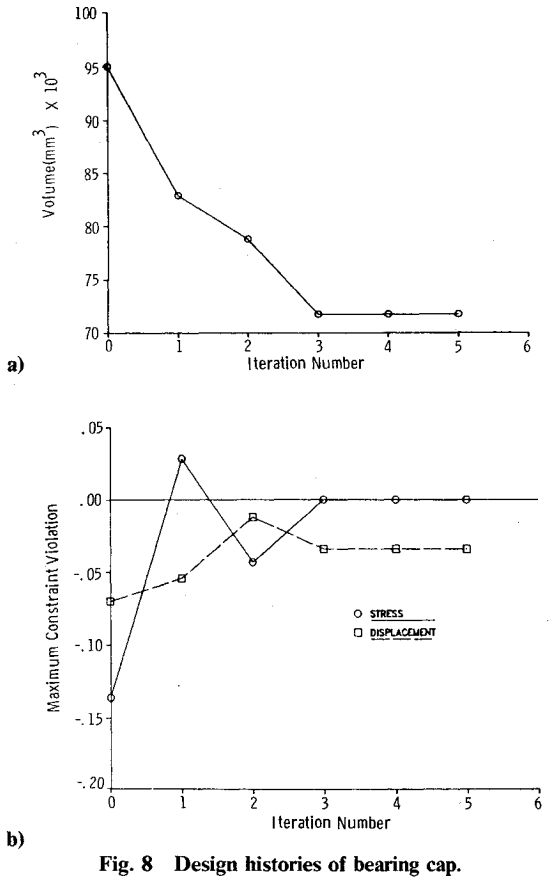

Fig. 8 Design histories of bearing cap.

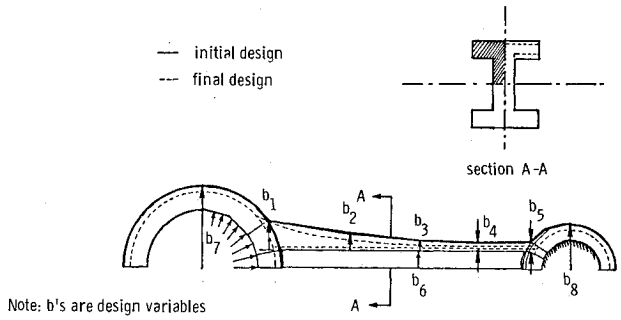

Fig. 9 Generic model of engine connecting rod.

critical yield stress used for analysis is chosen as 3000 MPa. Young's modulus and Poisson's ratio are 10.0×10^6 MPa and 0.3, respectively. The numerical data were selected for this example to demonstrate the use of the system and may not be realistic.

Using the symmetrical conditions, only a quarter of the structure needs to be analyzed. The generic model and design parameters are shown in Fig. 9. In this model, 8 design variables are chosen: 5 parameters define the shape of the shank and neck regions, 2 are the outer radii of the right and left holes, and 1 parameter defines the height of the web. The finite-element model, as shown in Fig. 10, contains 105 solid elements, 928 nodal points, and 2126 degrees of freedom.

The initial values of the design variables are shown in Table 3. Initially, the volume is 15686.7 mm^3 with no stress violation. After 20 design iterations, it is reduced to 7217.8 mm^3 with no stress violation. The final design variables and the final shape are shown in Table 3 and Fig. 9, respectively. Figure 11 shows the design history for the idealized connecting rod. In Fig. 11a, one observes that the convergence rate is reasonably good. From design iterations 10-17, the optimizer

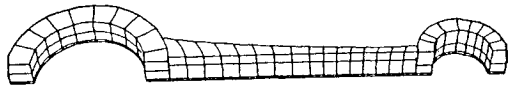

Fig. 10 Finite-element mesh of connecting rod.

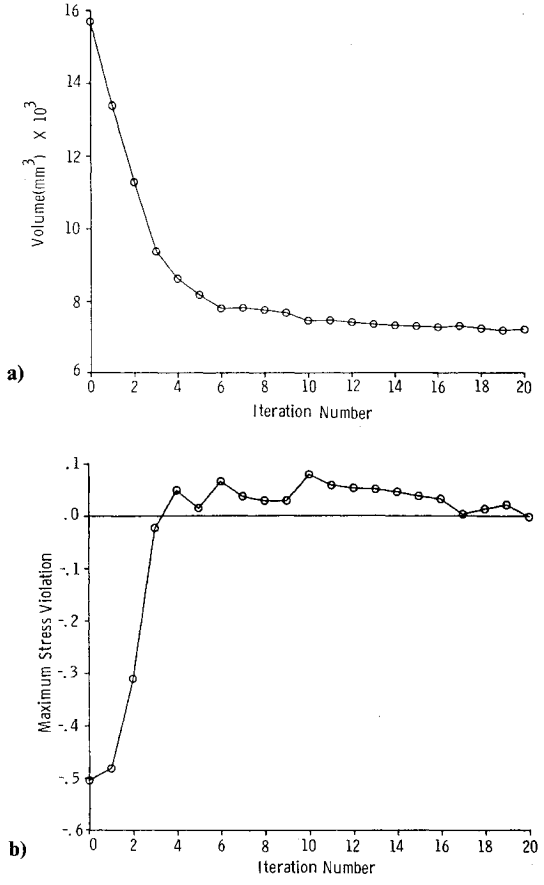

Fig. 11 Design histories of engine connecting rod.

tries to force the design into the feasible region. The slow correction for stress violation shown in Fig. 11b may result from Taylor's series expansion approximation for functions.

Summary

The development of a modular computer program for the shape optimization of three-dimensional solid components is discussed. The program uses NASTRAN for analysis and CONMIN for optimization. Since design sensitivities with respect to shape variables are not available in NASTRAN, a module had to be written to obtain these sensitivities, a module that is based on the material derivative concept applied to the variational state equation. Parameterized surface definitions and finite-element mesh generation were obtained from a module based on generic modeling concepts. Each program module is a separately executable program, but all modules can be executed sequentially using Job Control Language. Data communication between modules was handled using Fortran files. Several design examples have been provided to demonstrate the capabilities of the program.

References

[1]Imam, M.H., "Three-Dimensional Shape Optimization," *International Journal for Numerical Methods in Engineering*, Vol. 18, 1982, No. 5, pp. 661–673.

[2]Imam, M.H., "Minimum Weight Design of 3-D Solid Components,"*Proceedings of the Second International Computer Engineering Conference*, ASME, Vol. 3, San Diego, CA, Aug., 1982, pp. 119–126.

[3]Haug, E.J., Choi, K.K. Hou, J.W., and Yoo, Y.M., "A Variational Method for Shape Optimal Design of Elastic Structures," *New Directions in Optimum Structural Design*, edited by E. Atrek et al., Wiley, New York, 1984.

[4]Choi, K.K., and Haug, E.J., "Shape Design Sensitivity Analysis of Elastic Structures," *Journal of Structural Mechanics*, Vol. 11, No. 2, 1983, pp. 231–269.

[5]Haug, E.J., Choi, K.K., and Komkov, V., *Design Sensitivity Analysis of Structural Systems*, Academic Press, Orlando, FL, 1986.

[6]Yang, R.J. and Botkin, M.E., "Comparison Between the Variational and Implicit Differentiation Approaches to Shape Design Sensitivities," *AIAA Journal*, Vol. 24, June 1986, pp. 1027–1032.

[7]Botkin, M.E., "Shape Optimization of Plate and Shell Structures," *AIAA Journal*, Vol. 20, Feb. 1982, pp. 268–273.

[8]Goenka, P.K. and Oh, K.P. "A Three-Dimensional Mesh Generation Technique," Proceedings of the ASME Computers in Mechanical Engineering Conference, Las Vegas, NV, Aug. 12–16, 1984.

[9]Yang, R.J., Choi, K.K., and Haug, E.J., "Numerical Considerations in Structural Component Shape Optimization," *Journal of Mechanisms, Transmissions, and Automation in Design*, Vol. 107, Sept. 1986, pp. 334–339.

[10]Ramakrishnan, C.V. and Francavilla, A., "Structural Shape Optimization Using Penalty Functions," *Journal of Structural Mechanics*, Vol. 3, No. 4, 1974–1975, pp. 403–422.

[11]Yerry, M.A. and Shephard, M.S., "Automatic Three-Dimensional Mesh Generation by the Modified-octree Technique," *International Journal for Numerical Methods in Engineering*, Vol. 20, 1984, pp. 1965–1990.

[12]Vanderplaats, G., "CONMIN—A Fortran Program for Constrained Function Minimization User's Manual," NASA TM-X-62, 282, 1973.

[13]Yoo, Y.M. Haug, E.J., and Choi, K.K., "Shape Optimal Design of an Engine Connecting Rod," *Journal of Mechanism, Transmissions, and Automation in Design*, Vol. 106, Sept. 1984, pp. 415–489.

[14]Yang, R.J., Choi, K.K., and Haug, E.J., "Finite Element Computation of Structural Design Sensitivity Analysis," Univ. of Iowa, Iowa City, Rept. CCAD 84-3, 1984.